Bulgarian Journal of Agricultural Science, 26 (No 2) 2020, 309–322

Rice husk derived biochar as smart material loading nano nutrients and microorganisms

Ahmed Z. A. Hassan[1], Abdel Wahab M. Mahmoud[2*], Gamal M. Turky[3] and Gehan Safwat[4]

[1]*Agriculture Research Centre, Soil, Water& Environment Institute,12112, Giza, Egypt*
[2]*Cairo University, Faculty of Agriculture, Plant Physiology Department, 12613, Giza, Egypt*
[3]*National Research Centre (NRC), Dept. of Microwave Physics & Dielectrics, 12622, Giza, Egypt*
[4]*October University for Modern Sciences and Arts (MSA), Faculty of Biotechnology, 12588, Egypt*
[*]*Corresponding author:* mohamed.mahmoud@agr.cu.edu.eg

Abstract

Hassan, A. Z. A., Mahmoud, A. W. M., Turky, G. M. & Safwat, G. (2020). Rice husk derived biochar as smart material loading nano nutrients and microorganisms. *Bulg. J. Agric. Sci., 26 (2)*, 309–322

Present exploration aspired to produce biochar from rice husk basic nano particles using slow pyrolysis technique. The physio-chemical characteristics, phases and surface morphology of biochar were studied by different visual techniques.

The obtained result confirmed that rice husk derive biochar is considered as a novel carrier of nano nutrients and advantageous microorganisms. The recorded values of mean radius, nearest distance between particles, perimeter of particles, the surface area of biochar basic nano particles, cation and anion exchange capacity were examined. The image of surface topography showed that biochar enrich by nano-particles with "sponge" shaped structures and nano-particles were imbedded into macro, meso, and micro pores of biochar. The spacemen atoms of pure elements composition of biochar followed the descending order of oxygen > silicon > sodium > potassium > carbon > magnesium > calcium > alumina. The stability and fertility of biochar basic nano particles might be used as safety soil amendment, climate changes mitigation, source of fertilizer and eco-friendly. The determined conductivity of the prepared biochar is found in the range of semiconductors which make it suitable and promising material to be used as filler in polymer composites and nano composites for many electric and electronic applications.

Keywords: rice husk; biochar; microorganisms; dielectric spectroscopy

Introduction

Biochar is using in environmental management as it is considered a good sorbent for some contaminants, including heavy metals Biochar perhaps is well thought-out a unique landfill covers amendment for supported microbial methane oxidation due to its sorption properties, stability in soil and high internal micro-porosity Uchimiya et al. (2011). Moreover, biochar has gained more interest since it has considered carbon sequestration agent for enhance agricultural productivity Shackley et al. (2013). The post and production conditions controlled the physiochemical characteristics of the source materials and play important role in scheming properties of the resultant biochar Kloss et al., (2012). In addition, the temperature and duration of heat treatment are the key production calculating elemental composition of original feedstock composition. Increasing heat treatment realized an increase in surface area that improves the sorption of organic chemicals then carbonization degree of biochar increases subsequently decreased H: C and O: C ratios and amorphous organic matter contents Yu et al. (2009) and Uchimiya et al. (2011). Therefore, biochar might be used for environmental remediation since it reduced the bioavailability of toxic elements Yu et al. (2009).

Increased soil carbon sequestration can also improve soil quality because of the crucial role that C plays in chemical, biological and physical soil processes and many interfacial interactions Stevenson (1994). The biochar that remains consists mainly of many nutrients (C, N, Ca, K and P) increase soil nutrient levels and promote plant growth Glaser et al. (2002). The improving of soil fertility or increasing organic carbon yield relays on the physical and chemical properties of different feedstock and pyrolysis process. Infertile soils in different regions around the world have specific quality issues recommend that one biochar type will not solve all soil quality problems Lehmann et al. (2003).

On the other hand, biochar produced at lower temperatures (250-400°C) have higher yield recoveries and contains more C = O and C-H functional groups that can serve as nutrient exchange sites after oxidation Glaser et al. (2002). Moreover, biochar produced at these lower pyrolysis temperatures has more diversified organic character, including aliphatic and cellulose type structures. These may be good substrates for mineralization by bacteria and fungi which have an integral role in nutrient turnover processes and aggregate formation Alexander (1977), Thompson and Troeh (1978). Feedstock selection also has a significant influence on biochar surface properties and its elemental composition Glase et al. (2002), and Brewer et al. (2009).

Biochar improves soil quality through its effects on key soil processes. Many of the benefits of biochar were derived from its highly porous structure and associated high surface area. Generally, soil water holding capacity increases with its high porosity. Meanwhile, improve soil water retention and in rank shrink nutrient loss during leaching through the small pore spaces with positively charged surfaces Lehmann & Joseph (2009) and Verheijen et al. (2010). The common biochar inserts small amount of available nutrients to the soil which is considered a good soil conditioner, as divergent to a fertilizer Saran et al., (2009). Recently the broadband dielectric spectroscopy was employed to study the electrical and dielectric properties of the nano zeolite (NZ) particles converted from the rice husk with aluminum. The dielectric behavior of the rice husk derived biochar in comparison with that of the NZ looking for the optimization conditions for different application fields was studied by Hassan et al. (2017). The main components of the rice husk ash are silicon oxide (90-97%) with minor amounts of CaO, MgO, K_2O and Na_2O. The melting points of SiO_2, K_2O and Na_2O are 1410-1610, 350 and 1275°C, respectively. It was found that under high temperatures, oxides have low melting points with silica resulting glassy or amorphous materials which averted completion process of natural reactions on surface char from rice husk Anshu et al. (2004).

The performance of rice husk derived biochar in soil increased water holding capacity (WHC) reflect the decomposition processing of rice husk leading to increase soil organic matter which retained more soil moisture Varela et al. (2013).

The current research aims to rehabilitate rice husk derive biochar basic nano materials using low pyrolysis (350°C), identify by good quality physical and chemical properties, safety, affable flora and fauna with recover soil, plant and biology conditions along with reducing amount of soil input (organic or chemical fertilizers).

Materials and Methods

Rice husk was collected after harvesting season (September, 2016) from El-Sharkya province, Egypt and it cut into small parts then exposed to pyrolysis process in an oven at 100, 200, 300, and 350°C, for 24 hrs to get a biochar product. Rice husk was chemically analyzed (Table 1) according to Helrich (1990). Rock phosphate derived nano zeolite NZ RP [AM1], rice husk derived nano zeolite NZ RH [AM2] and feldspar derived nano zeolite NZ F [AM3] were mixed with biochar by weight ratio 1:100. The nano particles analyses are given in Table 2. The physic-chemical characteristics and surface morphology of the biochar product based nano particles were studied.

Table 1. The chemical analysis of used rice husk

SiO_2, %	Al_2O_3, %	Fe_2O_3, %	MgO, %	CaO, %	Na_2O, %	K_2O, %	P_2O_5, %	ZnO, %	MnO, %	TiO_2, %	SO_3, %
68	12.00	0.78	2.15	2.00	0.50	9.11	1.01	0.55	0.39	0.00	0.00

Table 2. The physical and chemical analysis of nano particles

Types of nano particles	Surface area, m^2/g	Mean radius, nm	Volume, nm^3	CEC, meq./g	AEC, meq./g
NZ RP(AM1)	1493	19.96	484600	32	4
NZ RH(AM2)	700	32.00	281074	45	1
NZ F (AM3)	713	41.oo	372449	37	3

NZ RP (AM1) = Rock phosphate derived nano zeolite, NZ RH (AM2) = Rice husk derived nano zeolite, NZ F (AM3) = Feldspar derived nano zeolite

The pH titration method was used to determine the cation and anion exchange capacity of the synthetic nano zeolites according to Hassan et al., (2017). Particle size distribution, mean radius, surface area and surface topology were measured using Atomic Force Microscopy (AFM) at Cairo Univ., Faculty of Science, Micro Analytical Center, atomic force lab. Water holding capacity was measured according to Hassan et al. (2017) and hydraulic conductivity was determined according to Klute (1965).

Electrical conductivity and dielectric dissipation factor are measured using a Novocontrol high resolution alpha dielectric analyzer, assisted by Quattro temperature controllers, using pure nitrogen as a heating agent and assuring temperature stability better than 0.2 K. The measurements are carried out at frequencies ranging between 100 mHz and 10 MHz and at different temperatures between 20 and 60°C. The specimens were compressed under 5 tons/cm^2 hydraulic pressure to form discs having a radius of 1.2 cm and a thickness of 0.2 cm. The measurements were conducted, using gold plated brass electrodes the first is of 10 mm in diameter, the second is of 20 mm in parallel plate capacitor configuration. The used dielectric system measures the complex dielectric function, ε*, which is equivalent to the complex conductivity function, σ* according to Moussa et al. (2017), Salwa et al. (2017), Kyritsis et al. (2009), Kremer & Schönhals (2002) even each of them describes different phenomenon. The relationship between both parameters can be expressed as:

$$\sigma^*(\omega,T) = i\varepsilon_o\omega\varepsilon^*(\omega,T), \text{ implying that } \sigma' = \varepsilon_o\omega\varepsilon'',$$

where ε_o the permittivity of the vacuum and ω is the radial frequency = 2πν. The used technique can be found in several new publications by detail.

Biochar elements were analyzed using atomic adsorption model (Pye Unicam, model SP-1900, US), Faculty of Agriculture Cairo University. Also, Zeta potential (ZP) was measured for biochar by Zeta-Meter 3.0+ system (Zeta Meter Inc., VA) at National Research Centre, Giza, Egypt.

Azotobacter chroococeom was provided by Microbiology Dept., Soil, Water and Env. Res. Inst., Agric. Res. Center (ARC), Giza, Egypt. Liquid cultures of *A. chroococeomm* (10^8 CFU/ml.) in 250 ml. Conical flasks were grown on modified Ashby's medium for five days at 28-30°C Abd El-Malak and Ishac (1968). Active strain of Bacillus megaterium was cultivated in 250 ml conical flasks containing 100 ml. Pikovskaya medium Pikovskaya (1984) for three days at 30°C, then strain enriched a nutrient broth medium for 48 hr. at 28°C to reach $1*10^8$ cell/ml. Difco Manual (1985). After preparation of the two strains, they mixed biochar basic nano particles with determine amount of the strain (*A.chroococcum* and *B. megaterium*) solution and observed the colonies growth of both strains for 24, 48 and 72 h then light microscopy was used to show the growth of the two strains inside macro, meso, and micro pores of biochar basic nano particles. EC and pH- meters were used to determined salinity and reaction of biochar.

Results and Discussion

Rice husk derived biochar basic nano particles size distributions

Atomic force microscope (AFM)

It can be evaluate variable nano particle geometry by using AFM, from established spherical nano particles to more mysterious fractal geometries of nano particle clusters as shown in Table 3 and Figures 1, 2 and 3. AFM is employed to investigate nano particle bodily properties such as size, and the critical entire bi and 3 dimensions structures of the nano particles. Additionally, critical sample image dimensions such as height, volume, surface area, and perimeter may be calculated and situated on viewed.

It was noticed that the average centre X and Y of biochar basic nano particles were 2.148 and 2.504 µm (Table 3). The recorded values of maximum, minimum, average, and average round Z were 0.594, 0.452, 0.533 and 0.516 µm, respectively. The recorded values of maximum diameter, pattern width, horizontal length, vertical length were 0.24, 0.155, 0.198 and 0.184 µm, respectively (Table 3). The radius as circle with or without hole and their mean recorded the same value (0.083 µm). The recorded values of mean radius variance, nearest distance between particles, perimeter of particles, C perimeter were 0.028, 0.127, 0.66 and 0.594 µm, respectively (Table 3). Moreover area excluding or including whole were registered equal value of 0.032 µm^2. In addition, the surface area of biochar basic nano particles has low value of 0.041 µm^2, with minimum volume value of 0.017 µm^3. The pattern particles direction and 2nd moment direction were 0.724 and 0.718 rad., respectively.

The circular, thin degree and roughness registered values of 1.966, 1.679, and 1.393 µm respectively. The represented data indicated that biochar can take delivery of nano-particles embedded on its spongy structure. This unique structure of the prepared biochar makes it promising advanced material for application in energy storage devices as electrodes as well as its applications as reinforcement filler in polymer composites. On one hand, its spongy character makes it of high specific surface area. Some kinds of biochar (e.g. wood

Table 3. Particle size distributions of rice husk derived biochar

Statistics Value	Center X, um	Center Y, um	Maximum Diameter, um	Pattern Width, um	Horizontal Fere Length, um	Vertical Fere Length, um	Radius as Circle excluding Hole, um	Radius as Circle including Hole, um	Mean Radius, um	Mean Radius Variance, um	Nearest Distance, um	Perimeter, um	C Perimeter, um	Maximum Z, um
Average	2.148	2.504	0.24	0.155	0.198	0.184	0.083	0.083	0.083	0.028	0.127	0.66	0.594	0.594
Standard Deviation	1.394	1.334	0.193	0.133	0.173	0.149	0.058	0.058	0.064	0.021	0.056	0.574	0.482	0.252
Line Average	3.053	3.215	0.395	0.269	0.349	0.305	0.124	0.124	0.132	0.044	0.152	1.159	0.985	0.7
Square Average	3.493	3.638	0.545	0.386	0.483	0.431	0.168	0.168	0.181	0.064	0.178	1.67	1.359	0.804
Cubic Average	3.753	3.892	0.675	0.496	0.593	0.557	0.212	0.212	0.226	0.081	0.204	2.131	1.689	0.891
Sum	1027	1197	114.5	74.01	94.75	87.71	39.53	39.54	39.76	13.5	60.72	315.4	284.1	283.7
Maximum	4.83	4.902	1.094	0.843	0.996	1.035	0.411	0.411	0.416	0.139	0.354	3.719	2.895	1.165

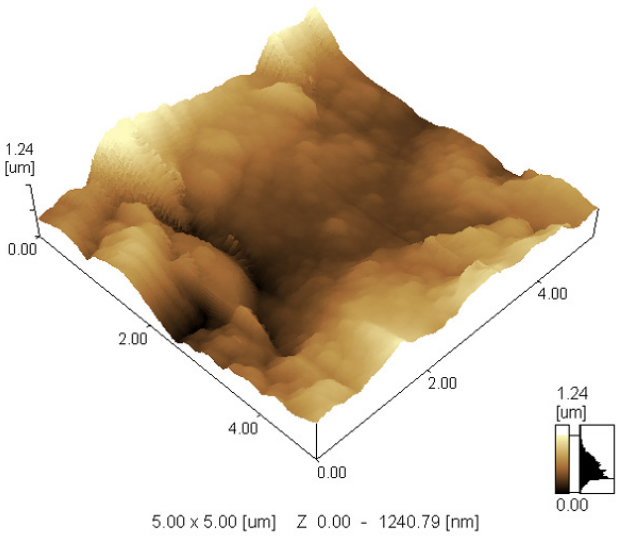

2D **3D**

Fig. 1. Images Bi & three dimensions of biochar (RH) embedded nano particles

ship biochar) have smaller pore size and higher pore volume revealed its benefit for filtration applications Ehsan Behazin et al. (2016), Koutcheiko & Vorontsov (2013).

The image of surface topography showed that biochar enrich by Nano-particles with "sponge" shaped structures and Nano-particles were imbedded into macro, meso, and micro pores of biochar basic Nano-particles (AM1, AM2 & AM3).

The recorded surface area of biochar basic nano particles was 0.041 μm^2. Biochar basic nano particles had negative zeta potential, reflecting a negative surface charge. These negative charges are responsible for cationic nutrients mechanism that adsorbed and retained by biochar basic nano particles. This mechanism lead to improved soil fertility in biochar amended soil Lehmann et al. (2006). During pyrolysis, the chemical characteristic of rice husk surface area derived biochar was affected by thermal alteration. The surface biochar serves as labile organic carbon while volatile matter that enrichment in many ionic species includes alkali metals is removed (Lehmann & Joseph, 2009).

The biochar pore volume (0.017 μm^3) and its roughness (1.393 µm) proofed its highly porous structure associated with high surface area. The mean radius of biochar basic nano particles (28 nm) reflected the contribution of nano particles mixed with biochar. The particle size distributions visibly forced hydraulic properties. Rice husk derived the finer biochar having inferior hydraulic conductivities attributable

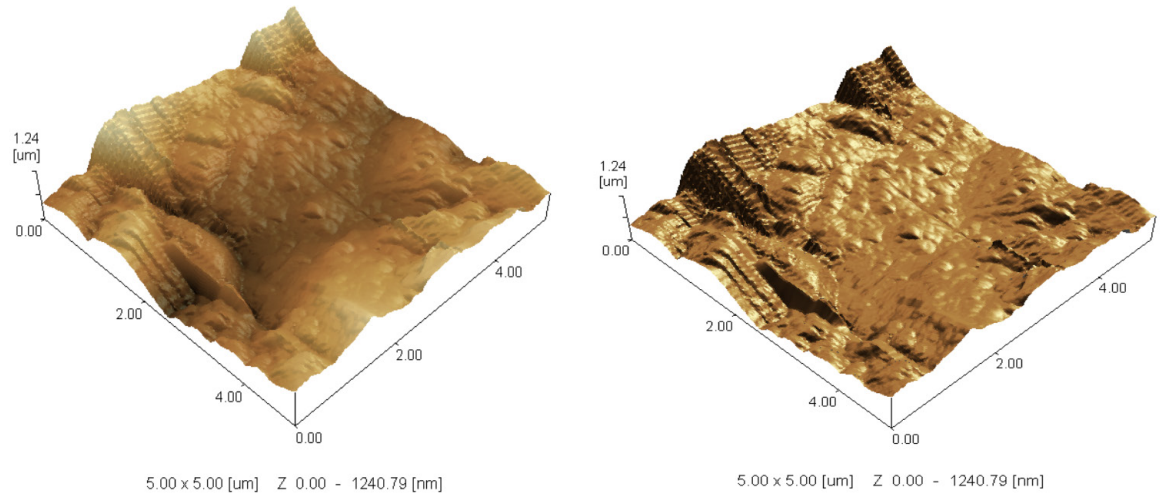

a *b*

Fig. 2. The three dimension images (a & b) of biochar basic nano particles

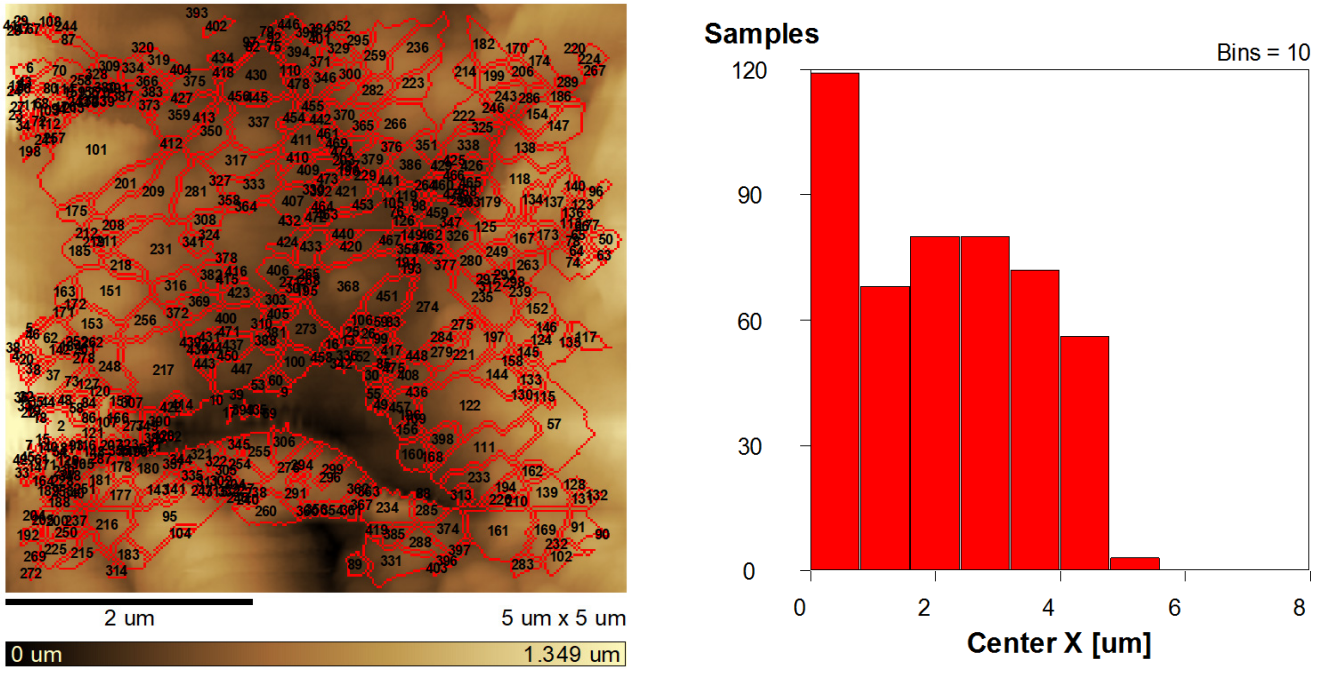

a *b*

Fig. 3. Particle analysis (*a*) and mean radius (*b*) of biochar basic nano particles

to lesser pore spaces. Simultaneously, upper water holding capacities were monitored in rice husk derived the finer biochar basic nano particles. These properties are together reflecting on sympathetic for soil enhancement. However, superior ash content biochar have minor fixed carbon and fairly high volatile matter contents, which led to subordinate their confrontation to biotic dilapidation and thus diminish their carbon sequestration potential (Lehmann & Joseph, 2009).

The metal oxides found in the ash fraction can react with the biochar to promote hasten its humiliation Huisman et al. (2012). Higher degradation rates of high ash biochar reflect its shorter lifetimes in natural soil systems. This exploration

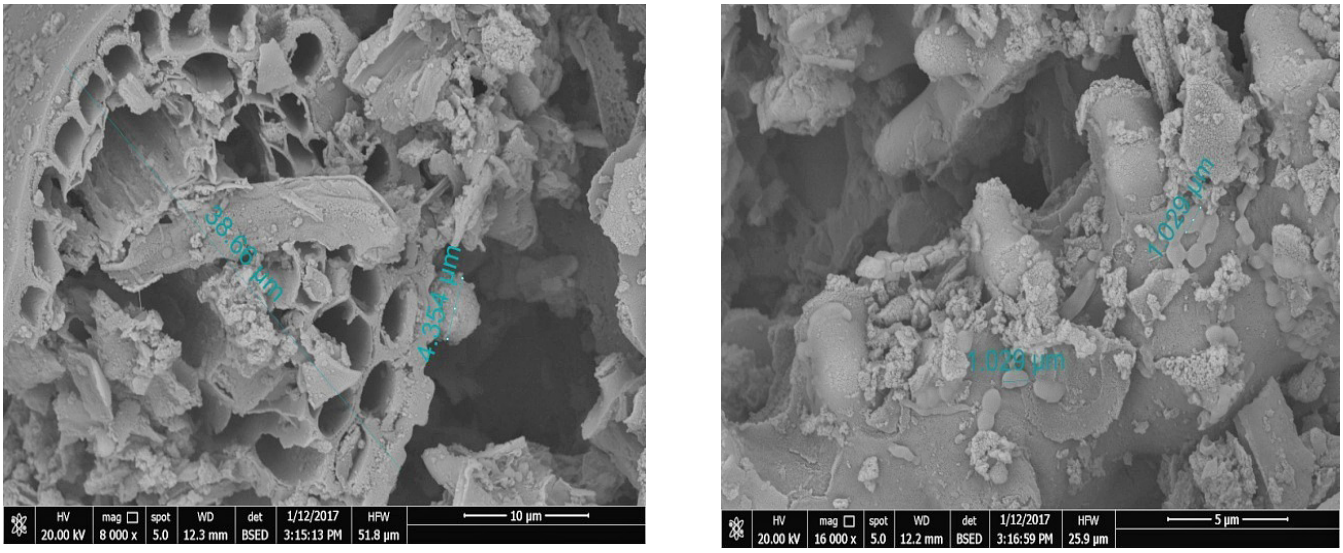

a *b*

Fig. 4. Image biochar basic nano particles after slow pyrolysis (350°C) and inoculation by microorganisms

aspired to produce biochar from rice husk basic nano particles using slow pyrolysis technique (350°C) in absence of oxygen with long term stability, the coverage of microbial utilization of the carbon in biochar and long lifetimes in natural soil systems.

The average value of dry density was 0.65 g cm^{-3}. This low dry density reflected the high internal porosity of rice husk derived biochar basic nano particles. The average specific gravity for biochar basic nano particles was high value (1.30) with low H: C ratio indicate that H: C can be charring intensity. This is a result of the heavier biomass components concentration (ash, metals and nano particles) generate from both positive degree of pyrolysis and nano particles imbedded biochar (Ameloot et al., 2013).

Scanning electron microscopy (SEM)

SEM images (Figure 4 a, b) were taken at different magnifications starting with 8000x and ending with 16000x. Visual scrutiny of Image (a) shows sponge shape and microstructure among biochar basic nano particles structure which has different sizes of pores. Moreover, porous structure of biochar including the nano particles was imbedded in biochar.

Visual scrutiny of Image (b) shows microstructure among biochar basic nano particles. Moreover, clearly confirm the porous structure of biochar including the cells of microorganisms (Azotobacter choroccocum and bacillus megiterium) with diameter of 1.299 µm. This finding led to verifying that biochar basic nano particles was organophillic and viewed as narrative carter of nano nutrients and advantageous microorganisms. Numerous of the reimbursement originated from highly porous structure of biochar and related high surface area. Biochar manufactured at low pyrolysis temperatures has more expanded organic character, counting aliphatic and cellulose form structures. These possibly good substrates for mineralization by microorganisms which has an essential responsibility in nutrient return processes first and second in aggregate formation (Brewer et al., 2009; Gaskin et al., 2008).

Energy dispersive elements (EDX)

EDX of biochar basic nano particles exemplify that the spacemen atoms of pure elements composition of biochar followed the descending order of oxygen > silicon > sodium > potassium > carbon > magnesium > calcium > alumina (Figure 5). The absence of nitrogen render to the low level concentration of nitrogen in rice hush in addition to the slow pyrolysis (350°C) of biochar led to loss nitrogen via volatilization process.

Specimen atoms pure elements of biochar basic nano particles and inoculated by two strains of microorganisms are shown in Figure 6. EDX of biochar basic nano particles epitomize that the spacemen atoms of pure elements composition of biochar inoculated by two strains of microorganisms were downward as follow: oxygen, carbon, silicon, sodium, nitrogen, boron, magnesium, aluminium, phosphorous and zircon. The nitrogen element percent (1.09%) as component in biochar analysis rendered to the success of Azotobacter

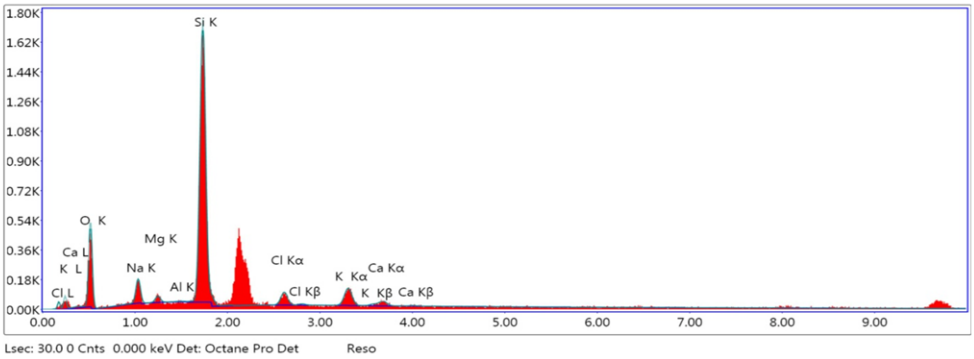

Element	Weight %	Atomic %	Net Int.	Error %
O K	39.93	54.27	80.82	10.97
NaK	6.84	6.47	30.32	10.96
MgK	1.3	1.16	9.31	17.99
AlK	0.09	0.07	0.77	80.04
SiK	41.42	32.06	421.4	4.28
ClK	3.32	2.04	22.93	16.26
K K	5.35	2.97	34.77	11.92
CaK	1.75	0.95	9.78	26.83

Fig. 5. Specimen atoms of biochar basic nano particles without inoculation by microorganisms

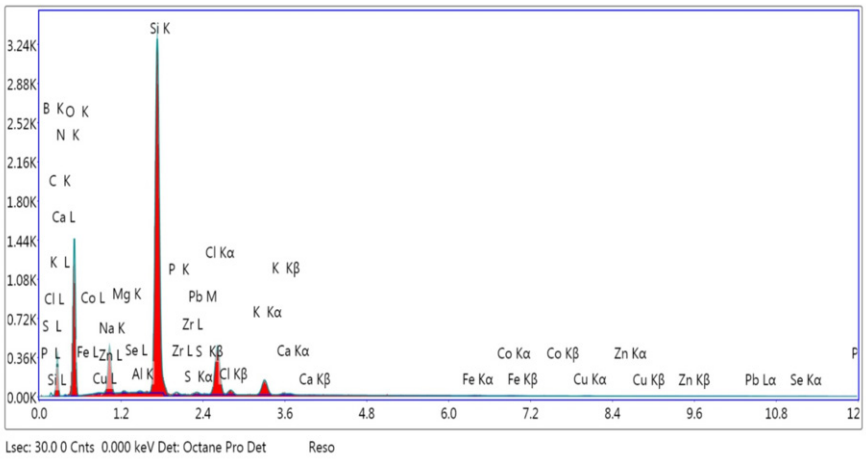

Fig. 6. Spacemen atoms pure elements of biochar basic nano particles with inoculation by microorganisms

chroccocum inoculation which fixed nitrogen inside and outside spongy structure of biochar.

Specimen atoms mapping of pure elements of biochar boosting nano particles after slow pyrolysis (350°C) process are shown Table 4 and Figure 7. Data registered that silicon was the major component of atoms followed oxygen, carbon, sodium, potassium, nitrogen, boron, magnesium, aluminium, phosphorous, calcium and zircon. In addition heavy metals were founded in trace amounts.

Table 5 give a picture of specimen atoms mapping of oxide elements of biochar boost nano particles after rehabilitation (slow pyrolysis 350°C) process. Data scheduled that carbon was the majority component of atoms followed by silicon, sodium, nitrogen, magnesium, sulphure, boron, aluminium, phosphorous and zircon. The presence of nitrogen oxide by 1.17% cause to be inoculated by *Azotobacter chroccocum* which fixed nitrogen inside biochar. In addition heavy metals were founded in trace amounts

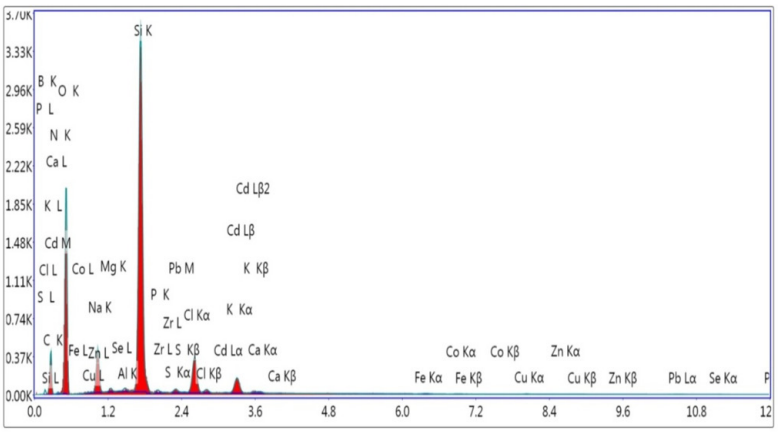

Fig. 7. Spacemen oxides of biochar basic nano particles and inoculation by microorganisms

Table 4. Spacemen atoms pure elements of biochar basic nano particles and inoculation by microorganisms

Element	Weight, %	Atoms, %	Net Int.	Error, %
B K	0.17	0.27	0.03	99.99
C K	23.33	34.23	39.32	12.91
N K	0.86	1.09	1.19	72.71
O K	37.76	41.59	204.29	10.24
Na K	4.85	3.72	66.73	9.7
Mg K	0.19	0.14	4.49	37.07
Al K	0.15	0.1	4.35	45.47
Si K	23.67	14.85	792.76	3.78
P K	0.11	0.06	2.44	66.61
Zr k	0.04	0.01	0.55	79.3

Table 5. Spacemen atoms of elements oxides of biochar basic nano particles and inoculation by microorganisms

Elements	Weight, %	Atomic, %	Net Int.	Error, %
B_2O_3	0.32	0.24	0.03	99.99
CO_2	48.6	58.15	43.14	12.34
N_2O_5	2.4	1.17	2	41.7
Na_2O	4.06	3.45	53.45	10.32
MgO	0.37	0.49	7.25	24.98
Al_2O_3	0.33	0.17	7.2	26.75
SiO_2	36.75	32.21	844.12	4.04
P_2O_5	0.27	0.1	4.3	30.96
ZrO_2	0.07	0.03	1.01	65.49
S_O3	0.45	0.3	7.38	69.91

Dielectric and Electrical analysis

The real part of complex conductivity was measured in siemens per centimetre and illustrated graphically against frequency in the range 0.1 Hz up to 10 MHz and at temperatures ranging from 20 to 60 in Figure 8. The considered biochar in this work has the conductivity varied between some orders of μS and mS per centimetre dependent on the frequency and temperature. This range of the conductivity of semiconductors just like the derived nano zeolite studied before. Regarding to these findings, biochar could be a suitable and promising material to be used as filler in polymer composites and nano composites. The enhancement of the electrical conductivity of the polymer composites using biochar as filler allows it for potential use in many technologies such as super-capacitors, sensors, batteries and many other electrical applications. This avoids many disadvantages in using carbon nanotube and graphene as fillers in that purposes such as high cost and poor dispersion in the polymer matrix (Othman et al., 2013; Nan Nan et al., 2016).

Moreover, there is a clear shoulder at the intermediate frequencies. It shifts to the lower frequency with heating. This assures that the spongy character of the biochar make it able to accumulate the charge carriers in the caves of the material. The expansion of the free volume with heating make it able to accumulate more and more charges which shifts the shoulder to the lower frequencies.

Figure 9 shows that the conductivity increases linearly with increasing temperature for both Biochar and nano zeolite (NZ) at least in the investigated temperature range. Generally it is clear that the conductivity of biochar and

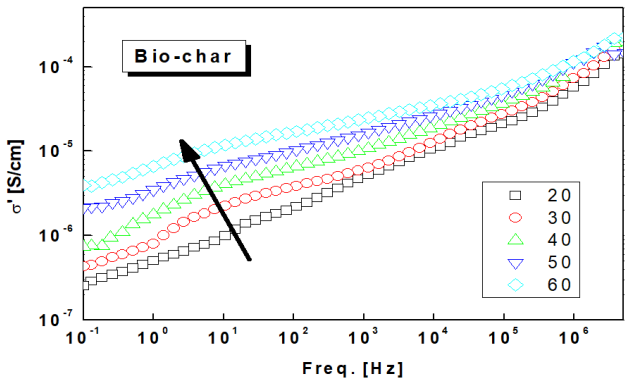

Fig. 8. The conductivity of *investigated* biochar in relation to the frequency at different temperatures

the rate of conductivity increasing with temperature are higher than that of NZ. This makes the prepared biochar more useful in enhancement of the electrical properties in addition to the tensile strength and thermal stability of polymers and rubbers (Layek et al., 2012; Peterson, 2012).

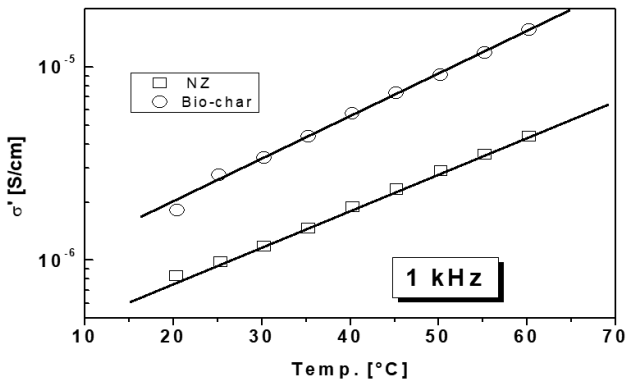

Fig. 9. The effect of temperature on the real part of Biochar conductivity and NZ at spot frequency point 1 kHz

The dielectric dissipation factor (tan δ = ε″/ε′) of the biochar is depicted against frequency at temperatures varied from 40 to 60°C in 5 C steps as shown in Figure 10. The main molecular dynamic peak was around 1kHz. The peak shifted very slowly with increasing temperature towards higher frequencies i.e. became a little bit faster with heating. There is also a remarkable increase of the peak intensity according to the increase of molecular group polarity that responsible for this dynamic.

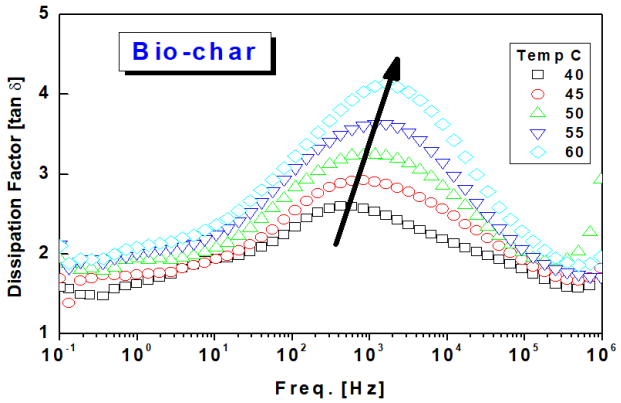

Fig. 10. The frequency effect on the dissipation factor at different temperatures

Biochar boosting nanoparticles

Biochar boosting nanoparticles were examined using transmission electron microscope (TEM) and their images are shown in Figure 11a, b, c, d. The magnification from 100000 x to 120000 x showed that the biochar basic nano particles has spongy structure embraced nano particles aggregates with different sizes.

The diameter of biochar basic nano particles in image C registered 84.9 nm comprise nano particles ranged between 15.1 - 16.3 nm. The image D recorded different sizes of biochar diameter (72.3-75.7 nm) embedded by nano particles size (14.2 nm). From images C and D, it can conclude that the nano particles impeded inside and outside biochar and it has different sizes (14.2, 15.1 and 16.3 nm). Moreover, biochar produced at this lower pyrolysis temperature has more diversified organic character, including aliphatic and cellulose type structures. These may be good substrates for mineralization by bacteria and fungi (Brewer et al., 2009), which have an integral role in nutrient turnover processes and aggregate formation (Gaskin et al., 2008).

The hydraulic properties of biochar basic nano particles including water holding capacity and hydraulic conductivity were determined and they are shown in Table 6. Water holding capacity of biochar was 60.9% from the total mass. On the dry weight basis, water holding capacity was 176.5%. The finer grained biochar led to higher water holding capacity. This may rendered to higher void ratios in finer grained of biochar basic nano particles moreover the stronger capillary forces among ultra fine particles of biochar basic nano particles. The biochar has a low value of hydraulic conductivity ($7.6*10^{-3}$ Kt cm/s), which it might be use for climate chang mitigation such as a land fill cover amendment, and it can pose a risk of excessive rainwater percolation and generation of leachate (Mukherjee et al., (2011).

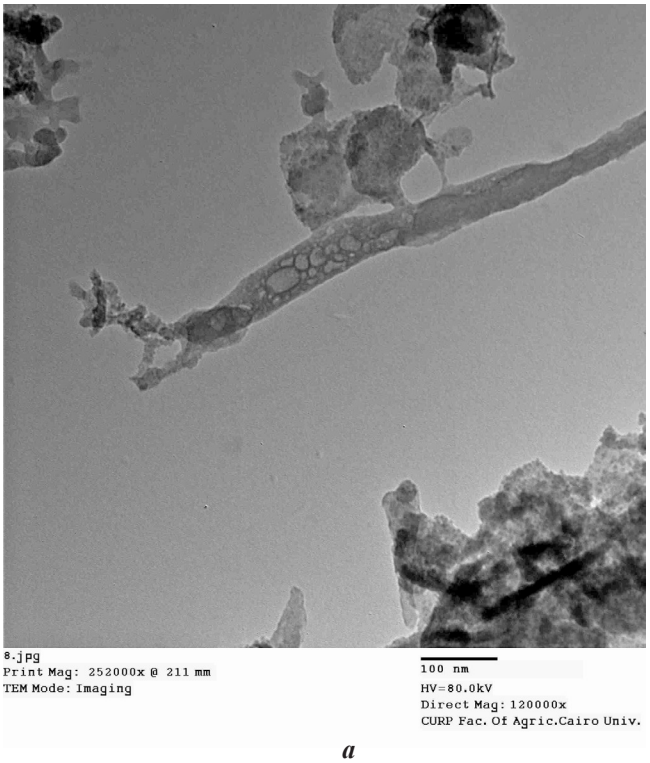

a

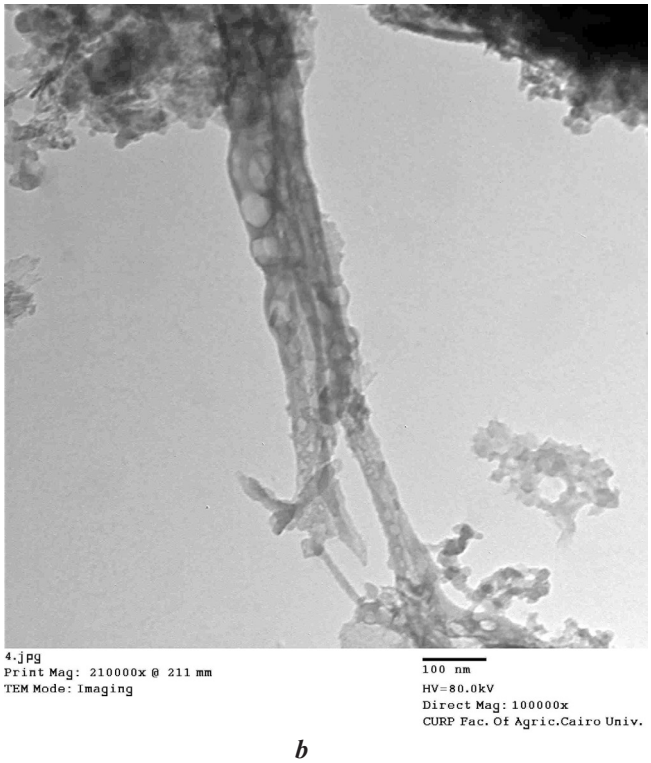

b

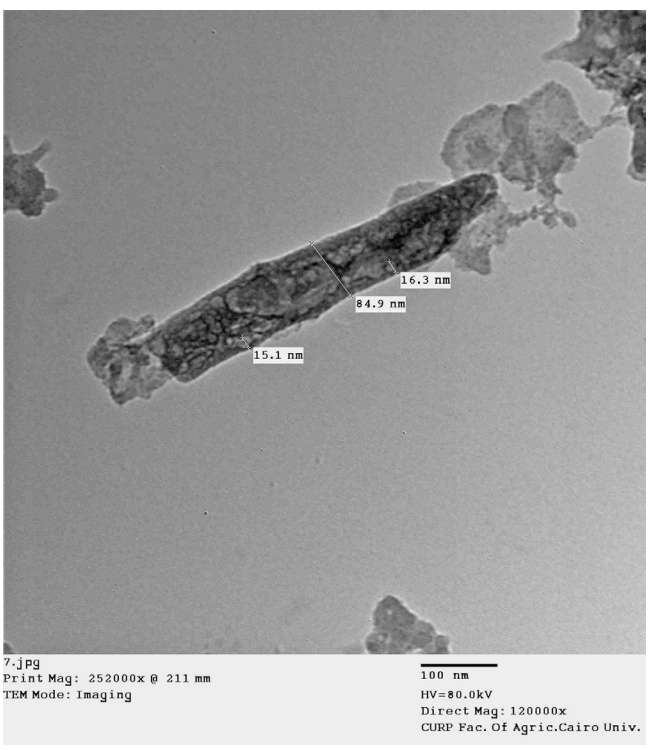

c

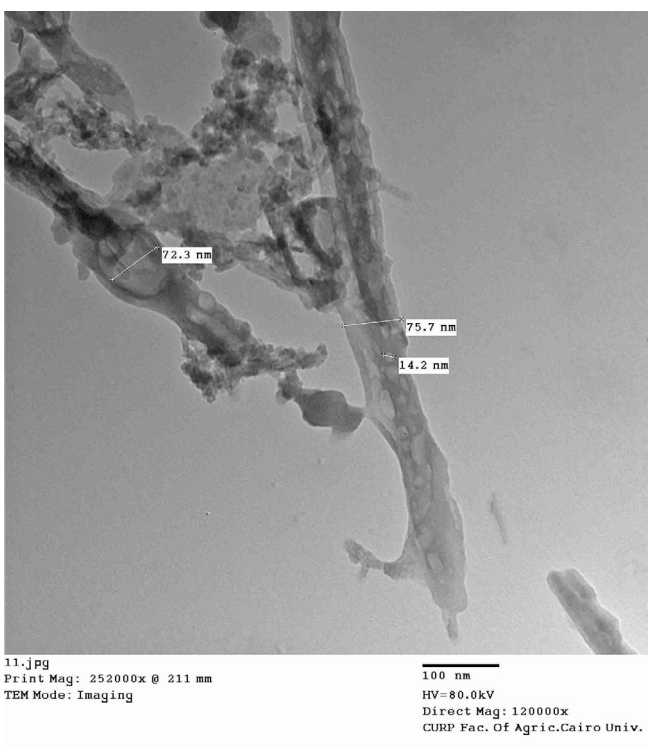

d

Fig. 11.The transmission electron microscope images (*a*, *b*, *c* and *d*) of biochar basic nano particles

Table 6. The hydraulic properties of rice husk derive biochar

Sample	Moisture content, %	Water holding capacity		Hydraulic conductivity Kt, cm/s
		Dry weight, %	Total mass, %	
Rice husk derive biochar	5.45	176.5	60.9	$7.6*10^{-3}$

The chemical composition of rice husk derive biochar basic Nano particles

The pH value of rice husk derives biochar by slow pyrolysis was slightly alkaline (7.45) with certain extent carbonization reflected by their lower H: C ratio (0.05). The extent of biomass pyrolysis is controlling the rise of alkaline pH due to its content of insoluble salts, which are more abundant in rice husk derive biochar (Brewer et al., 2009). The electric conductivity (EC) value of rice husk derive biochar is low (0.12 dS/ m) as shown in Table (7).

To assess the relative fractions of fixed and labile organic matter which represent by volatile matter component, gravimetric analysis of rice husk derive biochar was used. The values of fixed carbon (45.25%) and ash content (48.95%) refers to inorganic non combustible portion of rice husk derive biochar that remains after volatile matter removal by slow pyrolysis (350°C). It can be noticed that the higher fractions of ash content in rice husk derive biochar with slow pyrolysis seem to equalize with the higher value of fixed carbon. The chemical properties and compositions of rice husk attributes of the source materials. Moreover, variation in the relative amounts of ash and volatile matter as well as it has implications for biotic and abiotic interactions in biochar amended soil systems, namely the biochar long term stability and the extent of microbial utilization of the carbon in biochar (Spokas, 2010).

On the other hand, biochar produced at lower temperatures (350°C) have higher yield recoveries and contains more C = O and C-H functional groups that can serve as nutrient exchange sites after oxidation (Jeffrey & Ronald, 2002). Moreover, biochar produced at these low pyrolysis temperatures has more diversified organic character including aliphatic and cellulose type structures. These may be good substrates for mineralization by bacteria and fungi which have an integral role in nutrient turnover processes and aggregate formation (Brewer et al., 2009).

Both H = C and O = C ratios and analytical elements are valuable indicators of the quality of biochar Nguyen and Lehmann (2009). Rise in high temperature results in a superior loss of H and O compared to that of C. The dehydrogenation of CH_3 as a result of thermal stimulation indicates a change in the biochar recalcitrance (Harvey et al., 2012). In general, a biomass material typically involves labile and recalcitrant O fractions. The former is rapidly lost after the preliminary heating, while the final is retained in the char of the final product (Rutherford et al., 2012).

Table 7. The Chemical properties and composition of rice husk derive biochar

Elements	Rice husk derive biochar
Temperature, °C	350
Si, mg/kg	170
Ca, mg/kg	215
K, mg/kg	169
Mg, mg/kg	178
Water, %	3.8
Ash, %	48.95
pH	7.45
Fixed C, mg	45.25
H, mg	2.45
N, mg as N_2O after inoculation	2.4
N, mg as N_2O after soaking in ammonium sulphate	3.65
S, mg	0.20
O, mg	2.54
Volatile matter, %	----
H : C	0.05
C:N after inoculation by microorganism	18.85
C:N after soaking in ammonium sulphate	12.92
EC, dS/m	0.12
Zeta potential	-25.6 mV

The ratio of C: N after inoculation by microorganisms recorded 18.85. This value unsuitable for starting plant growth, while C: N ratio after soaking biochar in ammonium sulphate solution get optimum value (12.92) for sympathetic plant growth. Zeta potential value reflects surface charge of the material, was negative for the tested biochar basic nano particles, recorded (-25.6 mV). Zeta potential of biochar was significantly more negative, likely as a result of surface activation. A higher concentration of cationic metals may also contribute to the higher ZP of biochar.

Heavy metals concentrations in rice husk derive biochar

The heavy metals concentrations of biochar basic nano particles were under detection limits (Table 8). The major heavy metals were Fe, followed by Na, Mn, and Al. The minor heavy metals were Zn followed by Ni, Cu, Sr and Cr. In addition, the data pointed up the absence heavy metals were Pb, Cd, Sb and Sn.

Table 8. Heavy metals concentrations in rice husk derive bio-char

Fe, mg/l	Al, mg/l	Cu, mg/l	Pb, mg/l	Zn, mg/l	Cd, mg/l	Ni, mg/l	Cr, mg/l	Na, mg/l	Sb, mg/l	Mn, mg/l	Sn, mg/l	Sr, mg/l
8.56	1.05	0.08	---	0.8	----	0.12	0.04	7.20	-----	5.30	----	0.07

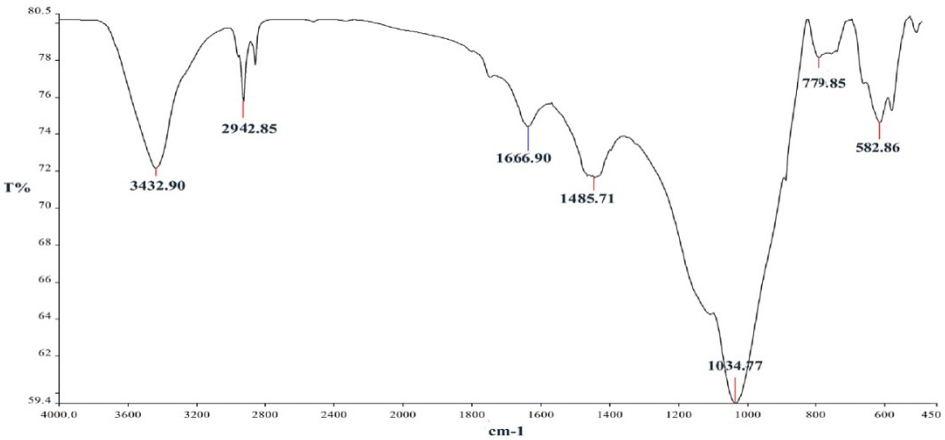

T – Transmission

Fig. 12. Infrared spectroscopy of biochar basic nano particles

Infrared spectroscopy (IR) of biochar basic nano particles

The calculated molar H/C ratio (0.05) for biochar basic nano particles guidance aliphatic as well as aromatic carbon compounds, among its minor H/C ratio, is possible to have extra aromatic carbon compounds. This judgment is sustained by the IR spectra of the biochar (Figure 12). Strong peak roughly (779.85/cm) narrates to aromatic CH out-of-flat surface bending vibration. It can be depicted that with slow pyrolysis peak temperature, the more aromatization was done. Constantly, biochar produced at these low pyrolysis temperatures has more diversified organic character, including aliphatic and cellulose type structures. These may be good substrates for mineralization by bacteria and fungi which have an integral role in nutrient turnover processes and aggregate formation (Brewer et al., 2009).

Cations and anions exchange capacity

Biochar has negative charge sites that magnetize and adsorb positive ions (the cations) like most soil particles. Characteristically, biochar added to clay or sandy soils sees CEC augment by ten, twenty or more points. The CEC of biochar boosting by nano particles has high CEC value (156.56 c mol/kg) attributed to the high values of CEC of nano particles enrich biochar. However, biochar has a further feature to dramatically boost its ion adsorption properties. The previous studies make known that biochar also has positive charges embedded in the bio-carbon matrix. This positive polarity magnetizes negative ions and molecules (the anions). These atoms are electron acceptors, and are charge carriers in cells to move energy around and deliver electric power to metabolic reaction sites. So, unlike most soil particles, biochar has anion exchange capacity (AEC). The two most critical soil anions are nitrogen and phosphorus, moreover nitrogen & phosphorus of N, P, fertilizers. These findings support that Biochar has potential within agro-ecosystems to be an N input, and a mitigation agent for environmentally detrimental N losses (Tim et al., 2013). The biochar boost by nano particles has AEC equal to 14.25 c.mol/ kg. This value was considered as a high AEC against many particles of soils due to participant of nano particles to raise this value. Anion adsorption is a powerful tool in soil fertility. By gathering and holding anions out of the soil solution, biochar immediately curbs leaching and loss of these nutrients. Instead of washing out with rain or irrigation, nitrogen, phosphorus, and other anions are held on and in the bits of biochar heighten by nano particles. On the supply side, this holds critical nutrients in the root zone and smart delivers more fertilizer to the plants, penetratingly increasing overall useful fertilizer efficiency.

Conclusion

The examined biochar for its properties and as a novel carter for two strains inoculants was success. Physical and

chemical properties of biochar were controlled by factors such as feedstock, slow pyrolysis temperature during production have been identified as affected biochar characteristics and its effectiveness as conditioner and fertilizer. Visual techniques were used such as high resolution (SEM) to prove that biochar can be loaded by nano particles and microorganisms. The chemical properties indicated the degree of carbonization of the biochar directly relates to its alkalinity which reflects high surface area. The electrical and dielectric properties of the rice husk derived biochar were investigated under very broad range of frequency and at different temperatures. The biochar is very promising in the polymer nano composite technology; not only as a reinforcement additive but also to enhance the electrical properties of the polymer matrix. Its conductivity in the range of the semiconductors makes it very applicable in many electrical and electronic devices. Biochar with high ash contents also tended to have greater amounts of trace metals, indicating the ash fraction of biomass is largely responsible for the presence of these constituents. Biochar can be safety tool used as adsorbent and carrier material for the two given microorganisms.

References

Abd El-Malak, Y. & Ishac, Y. Z. (1968) Evaluation methods used in counting Azotobacter. *J. Appl. Bact., 331*, 269-275.

Alexander, M. (1977). Introduction to soil microbiology. 2nd edn., John Wiley and Sons Inc.*,* New York, ISBN-13: 9780894645129, 467.

Ameloot, N., Graber, E. R., Verheijen, F. G. A. & De Neve, S. (2013). Interactions between biochar stability and soil organisms: review and research needs. *Eur. J. Soil Sci., 64*, 379–390.

Baldock, J. A. & Smernik, R. J. (2002).Chemical composition and bioavailability of thermally altered *Pinus resinosa* (Red pine) wood. *Organic Geochemistry*, *9(33)*, 1093–1109.

Behazin, E., Ogunsona, E., Rodriguez-Uribe, A., Mohanty, A. K., Misra, M. & Anthony, O. (2016). Mechanical, chemical, and physical properties of wood and perennial grass biochars for possible composite application. Anyia, *BioResources, 11*, 1334-1348.

Bharadwai, A., Wang, Y., Sridhar, S. & Arunachalam, V. S. (2004). Pyrolysis of rice husk. *Current Science, 87 (7),* 981-986.

Brewer, C. E., Schmidt-Rohr, K., Satrio, J. A. & Brown, R. C. (2009).Characterization of biochar from Fast pyrolysis and gasification systems. *Environ. Prog. Sustain. Energy, 28,* 386–396.

Clough, T. J., Condron, L. M., Kammann, C. & Müller, **Ch.** (2013). A review of biochar and soil nitrogen dynamics. *Agronomy, 3 (2),* 275-293.

Difco Manual (1985).Dehydrated culture media and reagents for microbiology. Laboratories Incorporated Detriot, Michigan, 48232 USA, 621.

El-Sabbagh, S. H., Ahmed, N. M., Turky, G. M. & Selim, M. M. (2017). Rubber nano-composites with new core-shell metal oxides as nano-fillers. Chapter 8, in [Progress in Rubber Nano composites], *A volume in Wood head Publishing Series in Composites Science and Engineering,* 249–283.

Gaskin, J. W., Steiner, C., Harris, K., Das, K. C. & Bibens, B. (2008). Effect of low-temperature pyrolysis conditions on biochar for agricultural use. Trans. *ASABE, 51,* 2061-2069.

Glaser, B., Lehmann, J. & Zech, W. (2002). Ameliorating physical and chemical properties of highly weathered soils in the tropics with charcoal-A Review. *Biol. Fertil. Soils, 35,* 219-230.

Harvey, O. M., Herbert, B. E., Kuo, L. J. & Louchouarn, P. (2012). Generalized two-dimensional perturbation correlation Infrared spectroscopy reveals mechanisms for the development of surface charge and recalcitrance in plant-derived biochars. *Environ. Sci. Technol., 46*, 10641–10650.

Hassan, A. Z. A., Wahab, A., Mahmoud, M. & Turky, G. (2017). Rice husk derived nano zeolite (A.M.2) as fertilizer, hydrophilic and novel organophillic material. *American Journal of Nano Materials, 5 (*1), 11-23.

Helrich, K. (1990). Official methods of analysis, 15th ed. Arlington, USA: Association of Official Agricultural Chemist. *1*, 673.

Huisman, D. J., Braadbaart, F., van Wijk, I. M., van Os & B. J. H. (2012). Ashes to ashes, charcoal to dust: micromorphological evidence for ash-induced disintegration of charcoal in Early Neolithic (LBK) soil features in Elsloo (The Netherlands). *J. Archaeol. Sci., 39*, 994–1004.

Kloss, S., Zehetner, F., Dellantonio, A., Hamid, R., Ottner, F., Liedtke, V., Schwanninger, M., Gerzabek, M. H. & Soja, G., (2012). Characterization of slow pyrolysis biochars: effects of feedstocks and pyrolysis temperature on biochar properties. *J. Environ. Qual., 41*, 990–1000.

Klute, A. (1965). Laboratory measurement of hydraulic conductivity of saturated soil. In: *Methods of soil analysis, Part I*, 210-221, Am.Soc.Agron. Inc. Publisher*,* Madison.

Koutcheiko, S. & Vorontsov, V. (2013). Activated carbon derived from wood biochar and its applications in super capacitors. *J. Biobased Materials Bioenergy, 7*, 733-740.

Kremer, F. & Schönhals, A. (2002). Broadband dielectric spectroscopy. Springer, Berlin, Germany.

Kyritsis A., Raftopoulos K., Abdel Rehim M., Shabaan Sh. Said, Ghoneim A. and Turky, G. (2009). Structure and molecular dynamics of Hyper Branched Polymeric systems with urethane and urea linkages. *Polymer, 50,* 4039.

Layek, R. K., Samanta, S. & Nandi, A. K. (2012). The physical properties of sulfonated graphene/ poly (vinyl alcohol) composites*. Carbon, 50*, 815–827.

Lehmann, J., da Silva, J. P. Jr., Steiner, C., Nehls, T., Zech, W. & Glaser, **B.** (2003). Nutrient availability and leaching in an archaeological anthrosol and a ferralsol of the central amazon basin: Fertilizer, manure and charcoal amendments. *Plant Soil, 249*, 343-357.

Lehmann, J., Gaunt, J. & Rondon, M. (2006). Biochar Sequestration in Terrestrial Ecosystems – A Review. *Mit. Adap. Stra. Global Change*, *11*, 395-419.

Lehmann, J. & Joseph, S. (2009). Biochar for Environmental Management: Science and Technology. Earthscan, London, UK. ISBN-13; 9781849770552, 416.

Milla, V. O., Rivera, E. B., Huang, W. J., Chien, C. C. & Wang, Y. M. (2013).Agronomic properties and characterization of rice husk and wood biochars and their effect on the growth of water spinach in a field test. *J. Soil Sci. and Plant Nutr., 13 (2),* 251-266.

Moussa, M. A., Ghoneim A. M., Abdel Rehim M. H., Khairy Sh. A. Soliman M. A. & Turky G. M. (2017). Relaxation dynamic and electrical mobility for polymethyl methacrylate - Polyaniline blends. *J. Appl. Polym. Sci.*, *134*, 45415-45425.

Mukherjee, A., Zimmerman, A. R. & Harris, W. (2011). Surface chemistry variations among a series of laboratory-produced biochars. *Geoderma*, *163*, 247–255.

Nan, N., Devallance, D., Xie, X. & Wang, J. (2015). The effect of bio-carbon addition on the electrical, mechanical, and thermal properties of polyvinyl alcohol/biochar composites. *Journal of Composite Materials*, *50 (9)*, 1161-1168.

Nguyen, B. T. & Lehmann, J. (2009). Black carbon decomposition under varying water regimes. *Org. Geochem., 40*, 846–853.

Othman, R. N., Kinloch, I. A. & Wilkinson, A. N. (2013). Synthesis and characterisation of silica–carbon nanotube hybrid microparticles and their effect on the electrical properties of polyvinyl alcohol composites*. Carbon, 60,* 461–470.

Peterson, S. C. (2012). Evaluating corn starch and corn stover biocharas renewable filler in carboxylated styrene–butadiene rubber composites. *J. Elastom. Plast., 44*, 43–54.

Pikovskaya, R. I. (1984). Mobilization of phosphorus in soil connection with the vital activity of some microbial species. *Microbiologya*, *17,* 362-370.

Rutherford, D. W., Wershaw, R. L., Rostad, C. E. & Kelly, C. N. (2012). Effect of formation conditions on biochars: compositional and structural properties of cellulose, lignin, and pine biochars. *Biomass Bioenerg., 46*, 693–701.

Saran, S., Lopez-Capel, E., Krull, E. & Bol, R. (2009). Biochar, climate change and soil: A review to guide future research. Corresponding author and editor: Evelyn Krull CSIRO Land and Water Science Report 05/09 February 2009.

Shackley, S., Sohi, S., Ibarrola, R., Hammond, J., Mašek, O., Brownsort, P., Cross, A., Prendergast-Miller, M. & Haszeldine, S. (2013). Biochar, tool for climate change mitigation and soil management. In: Lenton, T., Vaughan, N. (eds.), Geo-engineering responses to climate change. Springer, New York, 73–140.

Spokas, K. A. (2010). Review of the stability of biochar in soils: predictability of O:C molar ratios. *Carbon Manage*, *1,* 289–303.

Stevenson, F. J. (1994). Humus chemistry, genesis, composition, reactions, 2nd edn. John Wiley and Sons, Inc., New York, ISBN: 0471594741, 496.

Thompson, L. M. & Troeh, F. R. (1978). Soils and soil fertility, 4th edn. McGraw Hill, New York.

Uchimiya, M., Wartelle, L. H., Klasson, K. T., Fortier, C. A. & Lima, I. M. (2011). Influence of pyrolysis temperature on biochar property and function as a heavy metal sorbent in soil. *J. Agric. Food Chem*., *59*, 2501–2510.

Verheijen, F., Jeffery, S., Bastos, A. C., van der Velde, M. & Diafas, I. (2010). Biochar application to soils: A critical scientific review of effects on soil properties processes and functions. *JRC Scientific and Technical Research Series,* Italy.

Yu, X. Y., Ying, G. G. & Kookana, R. S. (2009). Reduced plant uptake of pesticides with biochar additions to soil. *Chemosphere, 76*, 665–671.

Received: June, 3, 2019; *Accepted:* August, 5, 2019; *Published:* April, 30, 2020